Division of Solid Mechanics

ISRN LUTFD2/TFHF-11/5163-SE(1-48)

Simulation and testing of crack sensitivity in TFA packaging material

Master thesis by
Oskar Karmlid

Supervisors
TeknD Ulf Nyman, Tetra Pak AB
Professor Per Ståhle, Div. of Solid Mechanics

For information, address:
Division of Solid Mechanics, Lund University
Box 118, SE-221 00 Lund, Sweden.
Homepage: http://www.solid.lth.se

Abstract

Tetra Paks package TFA, Tetra Fino Aseptic, is a cheap and thin package built of six layers of LDPE, paper board and aluminium, the market is mostly China and Africa. The material layers are connected with adhesion via the extruded LDPE. The geometry of the package causes left over material that creates folds in the package. The bad infrastructure in China and Africa expose the package for cyclic loading due to shake down which causes crack initiating and propagating in the folding area. If these cracks propagate through several layers the content can be exposed to oxidation and bacteria which can make it non-usable.

The purpose for this thesis is to investigate the mechanical properties of the packaging material, the reaction of the material when exposed to loading and the crack sensitivity coupled to the maximum strain in the material after loading. This investigation will be based on both physical experiments and numerical simulations in the Finite Element Method program ABAQUS. The simulations purpose is to get a better understanding of the different material parameters and the physical tests serves to verify the numerical model and to prove its credibility. The final model in ABAQUS will be used to test the parameters in an extensive parameter study with the ambition to find an ultimate combination of the parameters both for the material and the adhesion in the different layers.

The numerical model in ABAQUS is a two dimensional plane stress model because of the interest in maximum strain levels. The geometry is a 10 mm long material specimen which is folded and compressed between two plates with a clearance of 0.5 mm between them. The simulation uses a Dynamic Implicit solver with a quasi- static solution to enable damping through mass-scaling. The element type is a 4-node bilinear plane stress element with a linear order (in ABAQUS named CPS4) and full integration.

The physical test was made to fold the material and to expose it to extreme impact and to force it to fail. It was made after an unsuccessful bend test with a bend radius of 2 mm calculated from the theory behind composite beams. The fold tests geometry was also set to conform to the models geometry.

The verification of the model was successful both in the similarity of the reaction forces in the folding process and in buckling of the outside LDPE layer both seen in the simulation and in the microtome.

The ultimate case is to have a maximum reaction force to increase the fold stiffness in the material and to minimize the strain to reduce the risk for cracks in the aluminum. The parameter study shows that this seems to appear when there is extreme adhesion between the inside and the foil and with a stiffer inside LDPE. This combination seems to be the best solution to reduce cracks and big bend radius.

Acknowledgments

This thesis has been carried out at the platform New Material Design at Tetra Pak in Lund in cooperation with the Division of Solid Mechanics at the University of Lund, during February to June 2011.

I would like to thank my supervisor at Tetra Pak, Ulf Nyman, and other Tetra Pak employees Eskil Anderasson and Anders Harrysson for their help and support during my work. I would also like to thank Tetra Pak for their hospitality.

The Division of Solid Mechanics has been a great support during my M.Sc studies and my supervisor Per Ståhle has been a great coach and guide during my work with my master's thesis.

At least I would like to thank my friends and family for their stand-by and their consideration through out this spring.

Lund, July 2011

Oskar Karmlid

Nomenclature

TFA , Tetra Fino Aseptic
XFEM , Extended Finite Element Method
Adhesion , Describes the molecular bindings between two bodies closed in contact.
LDPE , Low Density Polyetylene

Contents

Chapter 1

Introduction

1.1 Tetra Pak

Tetra Pak is the world leader in food processing and packaging solutions. They provide safe and innovative packages for millions of peoples every day. Tetra Pak was founded by Ruben Rausing in Lund in the 1950's and his idea of tetraheredon shaped cartons for milk was borned. Today Tetra Pak is located in more than 170 countrys world wide.

The work of this thesis has been carried out in the group New Material Design at Tetra Pak in Lund, Ruben Rausings gata.

1.2 Aim of the thesis

(a) (b)

Figure 1.1: Tetra Fino Aseptic

TFA, Tetra Fino Aseptic, is a package from Tetra Paks platform Carton Econ-

omy. TFA is a packaging material laminate made out of Korsnas board, polymers and alu-foil. The TFA is usually used i China and Africa, providing cheap aseptic milk packaging. A large problem in these countrys is the infrastructure, this with the combination of old trucks results in big vibrations whitch leads to cyclic impact on the packages with cracks as a result. These cracks often appears in the same regions because of the geometry of the package, see figure **??** (b), the fold is where the crack initiates. This crack problem serves as the background for this master's thesis.

To understand the material and it differents parts the goal is to build a numerical crack model in ABAQUS. The modell is based on several layers of material which are assabled with cohesive zones between them. The cohesive zones purpose are to simulate the adhesion between the layers. To get cohesive zones whitch coincides with reality several, ordinary and some customized, adhesion tests has been carried out

The crack initiation and propagation are simulated with the Extended Finite Element Method and Linear Fracture Mechanics. The ambition is to first build a simplyfied modell with less material layers and only uniaxial simulation and to progress gradually when simulation and material behavior are verified.

The thesis will hopefully lead to further understanding of each of the laminates parts and how they contribute to crack developemnat in the laminate. Except the difference in material behavior adhesion and cohesion will also be investigated to gain further material understanding.

1.3 Limitations and assumptions

The limitation of a masters thesis is twenty weeks, to meet this deadline assumptions and limitations where necessary. Following list highlights and describes the assumptions and limitations.

- The original problem is a three dimensional, cyclic loading case where the package is exposed to impact during a long time. This complex loading case is hard to simulate which made it necessary to limit the simulations to a two dimensional, static loading case. This assumptions reduces the calculation time as well.
- Simplified material models. To reduce calculation time and to avoid many physical tests simplified material models were used, idel elastic or ideal elastic-plastic.
- The adhesion values in the simulation is based only on physical tests and calculations, no calibrations of the adhesion were done.
- Limited parameter study. A parameter study can be made very extensive, the study were limited to a few adhesive layers and material parameters.

New research areas can also be seen in Chapter 4, Results.

Chapter 2

Theory

This Chapter presents the essential theory needed to implement the method and to complete this master's thesis. For a deeper theory insight the reader is recommended to consult the bibliography.

2.1 Index notation

Matrix and tensor algebra results often in complex expressions and equations. Index notation can be used to reduce the complexity of these expresions. This section aims to inform and brief the reader in the definitions of index notation.

Index notation lies on a few definitions and conventions. The basis is the index of vetors and matrices. Vectors are written as

$$\boldsymbol{a} = a_i = \begin{pmatrix} a_1 \\ a_2 \\ a_3 \end{pmatrix} \tag{2.1}$$

and matrices are written as

$$\boldsymbol{B} = B_{ij} = \begin{pmatrix} B_{11} & B_{12} & B_{13} \\ B_{21} & B_{22} & B_{23} \\ B_{31} & B_{32} & B_{33} \end{pmatrix} \tag{2.2}$$

As one can see the index take the values $i = 1, 2$ and 3, this convention will follow thruout the whole report.

The summation convention reduces expressions and are defined by

$$b_i a_i = b_1 a_1 + b_2 a_2 + b_3 a_3 \tag{2.3}$$

Thus one can see if a index is repeated twice a sumation over this index appears.

The unit matrix is called Kronecker's delta in indexnotation language and are represented by a delta

$$\delta_{ij} = \begin{cases} 1 & if\ i = j \\ 0 & if\ i \neq j \end{cases} \tag{2.4}$$

To save space and effort one can write derivetives in an easy way in the index notation language as

$$\frac{\partial f}{\partial x_i} = f_{,i} \tag{2.5}$$

2.2 Continuum Mechanics

2.2.1 Large deformations

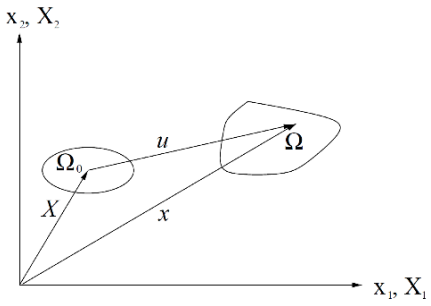

Figure 2.1: Deformation states [14]

To describe large deformations it is needed to formulate new strain measures. Figure 2.1 shows an undeformed body in the cartesian coordinate system $\boldsymbol{x_k}$. Its initial position vector for any material point in the undeformed state can be describe as

$$x_j^0 = x_k \boldsymbol{x_k} \tag{2.6}$$

The new material position vector, see figure 2.1, can be described with the displacements vector u_j as

$$x_j = x_j(x_j^0) = x_j^0 + u_j \tag{2.7}$$

Consider a vector between two material points in the same configuration. In the undeformed state this vector is given by dx_j^0 and dx_j in the deformed state. dx_j can be describe as

$$dx_i = F_{ij} dx_i^0 \tag{2.8}$$

where F_{ij} is the deformation gradient tensor

$$F_{ij} = \begin{pmatrix} \frac{\partial x_1}{\partial x_1^0} & \frac{\partial x_1}{\partial x_2^0} & \frac{\partial x_1}{\partial x_3^0} \\ \frac{\partial x_2}{\partial x_1^0} & \frac{\partial x_2}{\partial x_2^0} & \frac{\partial x_2}{\partial x_3^0} \\ \frac{\partial x_3}{\partial x_1^0} & \frac{\partial x_3}{\partial x_2^0} & \frac{\partial x_3}{\partial x_3^0} \end{pmatrix} \tag{2.9}$$

and

$$det(F_{ij}) > 0 \tag{2.10}$$

and thus the deformation gradient tensor is invertable.

From equation (2.27) it follows that F_{ij} can be described as

$$F_{ij} = \delta_{ij} + D_{ij} \tag{2.11}$$

Where δ_{ij} is the unit tensor and D_{ij} describes the partial derivatives of u_{ij}

$$D_{ij} = \begin{pmatrix} \frac{\partial u_1}{\partial x_1^0} & \frac{\partial u_1}{\partial x_2^0} & \frac{\partial u_1}{\partial x_3^0} \\ \frac{\partial u_2}{\partial x_1^0} & \frac{\partial u_2}{\partial x_2^0} & \frac{\partial u_2}{\partial x_3^0} \\ \frac{\partial u_3}{\partial x_1^0} & \frac{\partial u_3}{\partial x_2^0} & \frac{\partial u_3}{\partial x_3^0} \end{pmatrix} \tag{2.12}$$

The polar decomposition theorem says that F_{ij} can be separated into two components

$$F_{ij} = V_{ik} R_{kj} \tag{2.13}$$

where the symetric tensor V_{ik} represents the deformation and R_{kj} is an othorgonal tensor which describes the rotation.

2.2.2 Strain measure

Since this modelning involves large deformation and ABAQUS use Cauchy stresses (true stress) it is useful to take the logarithmic strain measure as default. The logarithmic strain measure is given by

$$\varepsilon_L = ln(V_{ik}) \tag{2.14}$$

2.2.3 Stress measures

It can be shown that stressstrain plots which uses logarithmic strain and Cauchy stresses coincide closely with test results [1]. Cauchy stress is also a measure that can be used for practical interest (traction carried out per unit current area), compared to other stress measurements. The Cauchy stress tensor σ_{ij}, or true stress, is defined by

$$t_i = \sigma_{ij} n_j \tag{2.15}$$

where t_i is the traction vector and n_j is outward normal vector [2].

2.3 Material behavior

The material is a laminate consisting of 6 different layers which in the simulations becomes 5 because the two inside LDPE layers are treated as one. The layers are compounded with adhesion which occurs when the LDPE are extruded on to the different parts.The figure bellow shows the construction of the laminate.

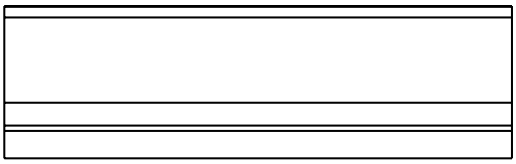

The attentive reflects over the modest thickness and do understand that this contribute to some difficulties in methods to actually see the crack and it's propagation.

The Board

Paper is a material of a special kind. Unlike steel paper behaves differently in different directions, this is because of the location of the cellulose fibers when the paper is produced. This manufacturing process leeds to the papers characteristic mechanical properties. This properties are based on three directions in the paper, see figure 2.2.

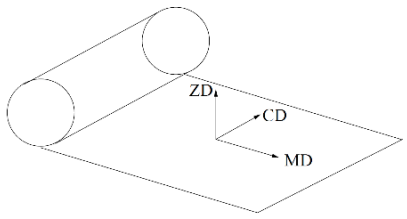

Figure 2.2: The directions in the board [14]

In these directions mechanical strength differs in a extensive manner with MD as the strongest direction and ZD as the weakest, ZD is drastically weaker than MD and CD because of the delamination risk of the paper.

2.3.1 Orthotropy

"If the constitutive relation takes the same form for every pair of Cartesian coordinate systems that are mirror images (reflections) of each other in a certain plane, this plane is a plane of elastic symmetry". Definition 4.50 in [2]

Hookes Law says

$$\sigma_{ij} = D_{ijkl}\epsilon_{kl} \tag{2.16}$$

A material with no symmtry planes is an anisotropic material. The constitutive matrix D_{ijkl} for an anisotropic material takes the form

$$\boldsymbol{D} = D_{ijkl} = \begin{pmatrix} D_{1111} & D_{1122} & D_{1133} & D_{1112} & D_{1113} & D_{1123} \\ D_{2211} & D_{2222} & D_{2233} & D_{2212} & D_{2213} & D_{2223} \\ D_{3311} & D_{3322} & D_{3333} & D_{3312} & D_{3313} & D_{3323} \\ D_{1211} & D_{1222} & D_{1233} & D_{1212} & D_{1213} & D_{1223} \\ D_{1311} & D_{1322} & D_{1333} & D_{1312} & D_{1313} & D_{1323} \\ D_{2311} & D_{2322} & D_{2333} & D_{2312} & D_{2313} & D_{2323} \end{pmatrix} \tag{2.17}$$

In a orthotropic material there exists two or three symmtery planes and D_{ijkl} takes the form

$$\boldsymbol{D} = \begin{pmatrix} D_{1111} & D_{1122} & D_{1133} & 0 & 0 & 0 \\ D_{2211} & D_{2222} & D_{2233} & 0 & 0 & 0 \\ D_{3311} & D_{3322} & D_{3333} & 0 & 0 & 0 \\ 0 & 0 & 0 & D_{1212} & 0 & 0 \\ 0 & 0 & 0 & 0 & D_{1313} & 0 \\ 0 & 0 & 0 & 0 & 0 & D_{2323} \end{pmatrix} \tag{2.18}$$

Many material shows an orthotropic behavior like paper, wood, rolled steel and aluminum [2].

2.3.2 Initial yield criterium

An initial yield criterium confirms if the material is affected with plastic deformation or failure. If the material is homogeneous the criteria only depends on the stress tensor σ_{ij} [2]

$$F(\sigma_{ij}) = 0 \tag{2.19}$$

If the material is anisotropic the criteria must depend also on a structural tensor.

$$\sigma_{ij}P_{ijkl}\sigma_{kl} - 1 = 0 \tag{2.20}$$

P_{ijkl} is a structural tensor and for a orthotropy material the tensor takes the form

$$\boldsymbol{P} = P_{ijkl} = \begin{pmatrix} F+G & -F & -G & 0 & 0 & 0 \\ -F & F+H & -H & 0 & 0 & 0 \\ -G & -H & G+H & 0 & 0 & 0 \\ 0 & 0 & 0 & 2L & 0 & 0 \\ 0 & 0 & 0 & 0 & 2M & 0 \\ 0 & 0 & 0 & 0 & 0 & 2N \end{pmatrix} \tag{2.21}$$

F, G, H, L, M and N are material parameters which characterize the orthotropy of the material just like the parameters in (2.18). These parameters can be determined by [2]

$$\begin{aligned} F &= \frac{1}{2}\left[\frac{1}{(\sigma_{yo}^{11})^2} + \frac{1}{(\sigma_{yo}^{22})^2} - \frac{1}{(\sigma_{yo}^{33})^2}\right] \\ G &= \frac{1}{2}\left[\frac{1}{(\sigma_{yo}^{11})^2} + \frac{1}{(\sigma_{yo}^{33})^2} - \frac{1}{(\sigma_{yo}^{22})^2}\right] \\ H &= \frac{1}{2}\left[\frac{1}{(\sigma_{yo}^{22})^2} + \frac{1}{(\sigma_{yo}^{33})^2} - \frac{1}{(\sigma_{yo}^{22})^2}\right] \\ L &= \frac{1}{2(\sigma_{yo}^{12})^2} \\ M &= \frac{1}{2(\sigma_{yo}^{13})^2} \\ N &= \frac{1}{2(\sigma_{yo}^{23})^2} \end{aligned} \tag{2.22}$$

Usually these parameters are nine but in this case it is only the deviatoric stresses that influence initial yielding [2].

With (2.21), (2.20) takes the form

$$F(s_{11}-s_{22})^2+G(s_{11}-s_{33})^2+H(s_{22}-s_{33})2+2Ls_{12}^2+2Ms_{13}^2+2Ls_{13}^2+2Ns_{23}^2-1=0 \tag{2.23}$$

s_{ij} is the deviatoric stress tensor defined as

$$s_{ij} = \sigma_{ij} - \frac{1}{3}\sigma_{kk}\delta_{ij} \tag{2.24}$$

(2.23) was proposed by Hill in 1950 and is called *Hill's Orthotropic yield criterion.*

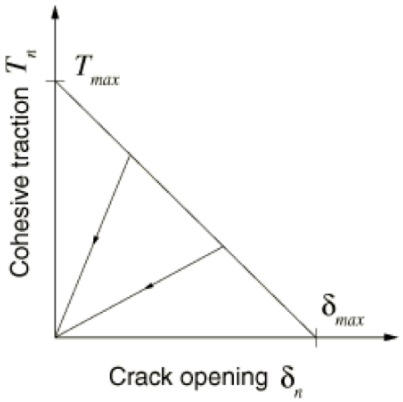

Figure 2.3: Cohesive separation law [12]

2.3.3 Adhesion and cohesive behavior

In many structures the use of adhesives is common. To describe the adhesive behavior one can use a separation law.

T_{max} is the maximum stress (Damage Initiation in ABAQUS) that the adhesive can take and δ_{max} (Damage Evolution in ABAQUS) is the maximum separation of the bulk material before the adhesive breaks and the bulk material are fully separated.

2.4 Nonlinear Finite Element Method

The Finite Element Method is a numerical method for solving partial differetial equations, developed by Olgierd Zienkiewicz.In solids mechanics these equations arise from the equation of motion. The weak form of the equation of motion is

$$\int_V \rho \boldsymbol{v}^T \ddot{\boldsymbol{u}} dV + \int_V (\tilde{\nabla}\boldsymbol{v})^T \boldsymbol{\sigma} dV = \int_S \boldsymbol{v}^T \boldsymbol{t} dS + \int_V \boldsymbol{v}^T \boldsymbol{b} dV \tag{2.25}$$

Where $\boldsymbol{v}$ is a arbitary weight function, ρ is the density, $\ddot{\boldsymbol{u}}$ the acceleration vector, $\boldsymbol{\sigma}$ the cauchy stresses, $\boldsymbol{t}$ the traction vector, $\boldsymbol{b}$ the body force and $\tilde{\nabla}^T$ an operator

$$\tilde{\nabla}^T = \begin{pmatrix} \frac{\partial}{\partial x} & 0 & 0 & \frac{\partial}{\partial y} & \frac{\partial}{\partial z} & 0 \\ 0 & \frac{\partial}{\partial y} & 0 & \frac{\partial}{\partial x} & 0 & \frac{\partial}{\partial z} \\ 0 & 0 & \frac{\partial}{\partial z} & 0 & \frac{\partial}{\partial x} & \frac{\partial}{\partial y} \end{pmatrix} \tag{2.26}$$

To reach the final FE-formulation some approximations are needed.

The displacement vector $\boldsymbol{u}$ is approximated with

$$\boldsymbol{u} = \boldsymbol{N}\boldsymbol{a} \tag{2.27}$$

Due to $\boldsymbol{a} = \boldsymbol{a}(t)$ it follows that

$$\ddot{\boldsymbol{u}} = \boldsymbol{N}\ddot{\boldsymbol{a}} \tag{2.28}$$

Where $\boldsymbol{N}$ is a vector whith the element shape functions, $\boldsymbol{a}$ is the nodal displacements vector and $\ddot{\boldsymbol{a}}$ is the nodal acceleration vector.

The weight function $\boldsymbol{v}$ is approximated with Galerkins method

$$\boldsymbol{v} = \boldsymbol{N}\boldsymbol{c} \tag{2.29}$$

Because $\boldsymbol{v}$ is arbitary $\boldsymbol{c}$ becomes arbitary as well.

$$\tilde{\nabla}\boldsymbol{v} = \boldsymbol{B}\boldsymbol{c} \tag{2.30}$$

where

$$\boldsymbol{B} = \tilde{\nabla}\boldsymbol{N} \tag{2.31}$$

With (2.28)-(2.31), (2.25) takes the form

$$\boldsymbol{c}^T \left((\int_V \rho \boldsymbol{N}^T \boldsymbol{N} dV)\ddot{\boldsymbol{a}} + \int_V \boldsymbol{B}^T \boldsymbol{\sigma} dV - \int_S \boldsymbol{N}^T \boldsymbol{t} dS - \int_V \boldsymbol{N}^T \boldsymbol{b} dV \right) = 0 \tag{2.32}$$

As a result of $\boldsymbol{c}$ being arbitrary (2.32) reduces to

$$\boldsymbol{M}\ddot{\boldsymbol{a}} + \int_V \boldsymbol{B}^T \boldsymbol{\sigma} dV = \int_S \boldsymbol{N}^T \boldsymbol{t} dS + \int_V \boldsymbol{N}^T \boldsymbol{b} dV \tag{2.33}$$

Where $\boldsymbol{M}$ is the mass matrix

$$\boldsymbol{M} = \int_V \rho \boldsymbol{N}^T \boldsymbol{N} dV \tag{2.34}$$

The other parts of (2.33) are defined as

$$\boldsymbol{f}_{int} = \int_V \boldsymbol{B}^T \boldsymbol{\sigma} dV \tag{2.35}$$

$$\boldsymbol{f}_{ext} = \int_S \boldsymbol{N}^T \boldsymbol{t} dS - \int_V \boldsymbol{N}^T \boldsymbol{b} dV \tag{2.36}$$

$\boldsymbol{f}_{int}$ are the internal forces and $\boldsymbol{f}_{ext}$ are the external forces. With these definitions the finial dynamic FE-Formulation is reached

$$\boldsymbol{M\ddot{a}} = \boldsymbol{f}_{ext} - \boldsymbol{f}_{int} \tag{2.37}$$

For further information about the Finite Element Method see [1] and [10].

2.4.1 Extended Finite Element Method

The Extended Finite Element Method is an extended version of the ordinary Finite Element Method. XFEM is extended in a way that allows it to treat discontinuities and singularities, this qualification is useful to simulate crack initiation and propagation.

In the Finite Element Method the element boundaries are described by element shape functions. These functions are often polynomials and can not treat discontinuities. Is is in this area of the method where it has bin extended. The XFEMs element shape functions are extended in a way so that the functions can hold discontinuities. This extension is based on a partion of unity [3], this allows local enriched functions to be included in a finite element approximation.

The enriched funtions consists of near-tip asymptotic functions which captures the sengularities och discontinuities near the crack tip. The displacement vector $\boldsymbol{u}$ is enriched with partion of unity [3]

$$\boldsymbol{u} = \sum_{i=1}^{N} N_i(x) \left[\boldsymbol{u}_i + H(x)\boldsymbol{a}_i + \sum_{\alpha=1}^{4} F_\alpha(x)\boldsymbol{b}_i^\alpha \right] \tag{2.38}$$

N is the element shape function, H is the associated discontinous jump function, $\boldsymbol{a}$ is the nodal enriched degree of freedom vector, F is the associated elastic asymptotic crack-tip functions for a isotropic elastic material and $\boldsymbol{b}$ is the nodal enriched degree of freedom vector. F and H is defined as

$$F_\alpha(x) = \left[\sqrt{r}sin\frac{\theta}{2}, \sqrt{r}cos\frac{\theta}{2}, \sqrt{r}sin\theta sin\frac{\theta}{2}, \sqrt{r}sin\theta cos\frac{\theta}{2} \right] \tag{2.39}$$

$$H(x) = \begin{cases} 1 & if(\boldsymbol{x} - \boldsymbol{x}^*)\boldsymbol{n} \geq 0 \\ -1 & otherwise \end{cases} \tag{2.40}$$

(r, θ) is a polar coordinate system with its origin located at the crack tip front, $\boldsymbol{x}$ is a Gauss point, $\boldsymbol{x}^*$ is a point on the crack closest to $\boldsymbol{x}$ and $\boldsymbol{n}$ is the normal to the crack at $\boldsymbol{x}^*$

Asymptotic crack-tip functions is only used when modeling stationary cracks in ABAQUS/Standard. When modeling moving cracks one just need to consider the displacement jump across a cracked element i considered.

2.5 Numerical Solution for Non Linear Dynamics

A common operator for Non Linear Dynamics is the Newmark operator, the operator Hilber-Hughes-Taylor is a generalized version of the Newmark operator with controllable numerical damping [12]. This damping is coveted inte the automatic time stepping scheme, where often high-frequency numerical noise appear. The Hilber-Hughes-Taylor operator replace (2.33), the equation of motion, with

$$\boldsymbol{M}\ddot{\boldsymbol{u}}|_{t+\Delta t}+(1+\alpha)(\boldsymbol{f}_{int}|_{t+\Delta t}-\boldsymbol{f}_{ext}|_{t+\Delta t})-\alpha(\boldsymbol{f}_{int}|_{t}-\boldsymbol{f}_{ext}|_{t})+\boldsymbol{L}^n|_{t+\Delta t}=0 \quad (2.41)$$

Where t is the actual time step, $t+\Delta t$ is the next time step and $\boldsymbol{L}^n$ is the sum of all Langrange multiplier related to n degrees of freedom. The Hilber-Hughes-Taylor operator is completed with the Newmark formulae for the displacement and the velocity [12]

$$\boldsymbol{u}|_{t+\Delta t}=\boldsymbol{u}|_t+\Delta\dot{\boldsymbol{u}}|_t+\Delta t^2((\frac{1}{2}-\beta)\ddot{\boldsymbol{u}}|_t+\beta\ddot{\boldsymbol{u}}|_{t+\Delta t}) \quad (2.42)$$

$$\dot{\boldsymbol{u}}|_{t+\Delta t}=\dot{\boldsymbol{u}}|_t+\Delta t((1-\gamma)\ddot{\boldsymbol{u}}|_t+\gamma\ddot{\boldsymbol{u}}|_{t+\Delta t}) \quad (2.43)$$

With values for the constans as

$$\beta=\frac{1}{4}(1-\alpha)^2 \quad (2.44)$$

$$\gamma=\frac{1}{2}(1-\alpha) \quad (2.45)$$

$$-\frac{1}{3}\leq\alpha\leq 0 \quad (2.46)$$

The oprators strenght is the damping it posses and that the energy dissipation is always small, not more than 1 % of the systems total energy [12]. For further information about Numerical Solutions for Non Linear Dynamics see [1].

2.6 Fracture Mechanics

All materials and structures contains cracks. Fracture Mechanics is the theory of these cracks, their initiation and their propagation. There exist three basic modes of crack tip loading [7]. These three modes can be seen in figure 2.4.

In Linear Elastic Fracture Mechanics it is assumed that the material can be described with only Linear Elastic Isotropic Theory [11]. The condition at the crack tip can then be described by the stress-intensity factors K_I, K_{II} and K_{III}. These factors are defined as [11]

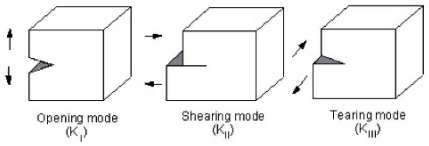

Figure 2.4: The three basic modes of fracture [13]

$$K_I = \lim_{x \to +0} \sigma_y(x,0)\sqrt{2\pi x} \tag{2.47}$$

$$K_{II} = \lim_{x \to +0} \tau_{xy}(x,0)\sqrt{2\pi x} \tag{2.48}$$

$$K_{III} = \lim_{x \to +0} \tau_{yz}(x,0)\sqrt{2\pi x} \tag{2.49}$$

From these equations one can see that σ_x, τ_{xy} and $\tau_{yz} \to \infty$ when $x \to +0$.

There are several ways of calculating these factors, for more information see [7] and [11].

Energy flow at the crack tip

A central section in fracture mechanics is the amount of energy transported to the crack tip, denoted G, and how much energy is needed for the crack tip to propagate. In linear elastic systems the following relation holds [7]

$$G = \frac{K_x^2}{E'} \tag{2.50}$$

where E' is the Youngs modulus is defined as

$$E' = \begin{cases} \frac{E}{1-\nu^2} & planestrain \\ E & planestress \end{cases} \tag{2.51}$$

In the general case the energy flow can be calculated with the J-integral [11], a line integral around the crack tip.

$$J = \int_\Gamma \left(A'dy - \sigma_{ij} n_j \frac{\partial u_i}{\partial x} ds \right) \tag{2.52}$$

Where Γ is the path which is integrated, σ_{ij} the stress tensor, n_j the outer normal to the integrate path, u_i the displacement discontinuity and A'

$$A' = \int \sigma_{ij} d\varepsilon_{ij} \tag{2.53}$$

is the deformation work per volume unit.

Fracture Criteria

As a definition for when crack initiation occurs the property fracture thoughness is introduced [7]. Crack initiation occurs when

$$G \geq G_{cr} \tag{2.54}$$

Where G_{cr} stand for the critival fracture energy.

Chapter 3

Method

This Chapter is a description of the methods used to implement this master's thesis. Every stage in the work process can be read in this chapter, and the ambition is that that reader can apply the same methods after the reading. The first part describes how the physical tests has been made then the method for building the model, with the physical parameters, in ABAQUS is described. Each of the steps made in ABAQUS is outlined so that the reader is able to implement this kind of simulation.

3.1 Physical Tests

To verify the final model in ABAQUS and to investigate material behavior some physical tests was carried out.

3.1.1 Adhesion

To get real parameters that ABAQUS requires for the cohesive behavior physical adhesion tests where performed, some made after Tetra Pak standards and some customized. A common test for adhesion is the peel test, figure 3.1. Tests performed for this thesis are all peel tests with different peel angels, θ.

In procedure provided by Kinloch [8] one calculate the fracture energy G_C and maximum principal stress σ_{max} for different peel angels. To compare results, when it was feasible, both $\theta = 90^o$ and $\theta = 180^o$ was performed. Because of the modest thickness of the material some of the adhesion layers could not be measured. The problem was either that it was too thin or that the paper delaminated insted of adhesion layer breakage. From Kinloch's procedure [8] the most interesting outputs needed for ABAQUS is the critical fracture energy G_C and maximum principal stress that the adhesion layer can suffer σ_{max}. These parameters for the different layers can be seen i the following table l.

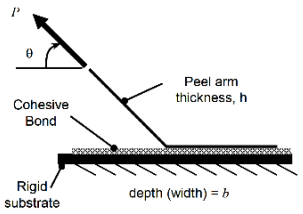

Figure 3.1: The Peel test [6]

Layer	G_C J/m^2	σ_{max} (MPa)
Inside/Foil $\theta = 180^o$	303.5	615.7
Inside/Foil $\theta = 90^o$	272.5	583.4
Decour/Paper $\theta = 180^o$	222.5	527.2
Lam/Foil $\theta = 180^o$	160	447

How the different θ peel tests were performed and how the set up was can be seen in figure 3.2.

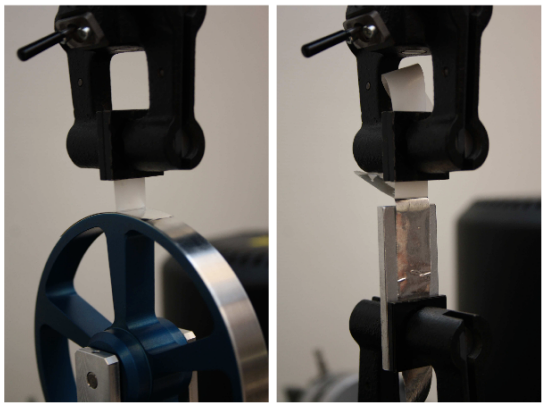

(a) 90^o (b) 180^o

Figure 3.2: The different Peel tests

3.1.2 Test of adhesion between shear and normal forces

To investigate the relation between adhesion in shear and normal direction tensile tests were carried out in the different directions. The tests was easily made out of two pieces of TFA material which were compound with a piece of iron and a hot iron, see figure 3.3a. The test was then performed in a tensile machine either in the shear direction, figure 3.3b, or in the normal direction, figure 3.3c.

The machine that was used for the test is an Zwick/Roell Z010, see figure 3.4

for machine and clamps.

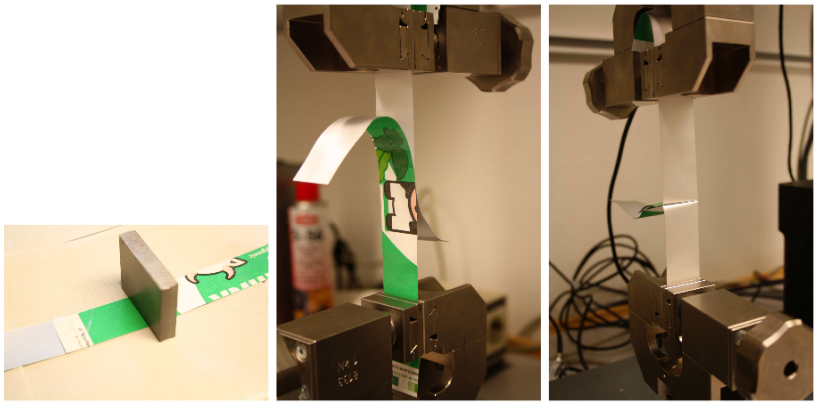

(a) Compund of TFA (b) Shear direction (c) Normal direction

Figure 3.3: Set up for Shear vs. Normal Adhesion

When test was performed in the shear direction the TFA material did break before the adhesion layer was damaged. In the normal direction the board dilaminated instead of the adhesion layer did break. Whith this insight and discussion with Prof. Per Ståhle at the Division of Solid Meachanics, Lund University and Johan Tryding, Tetra Pak, a factor of ten (10) was determined. The adhesion in the shear direction was set to be ten times stronger than in the normal direction. This relation is used when the cohesive surfaces is implemented in ABAQUS.

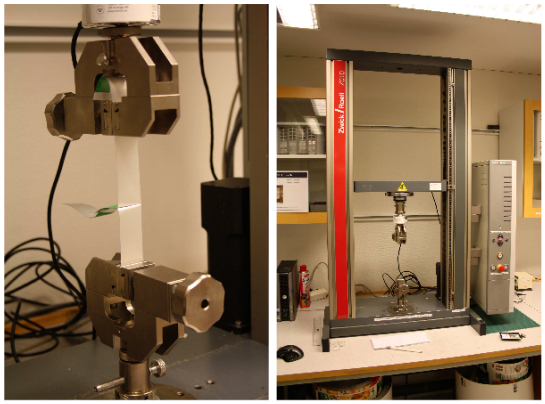

(a) The Clamps (b) The Tensile Machine

Figure 3.4

3.1.3 Bend Test

To investigate how a real crack initiates and propagates a customized test was proposed. A bend test was the load case closest to the real case but not to

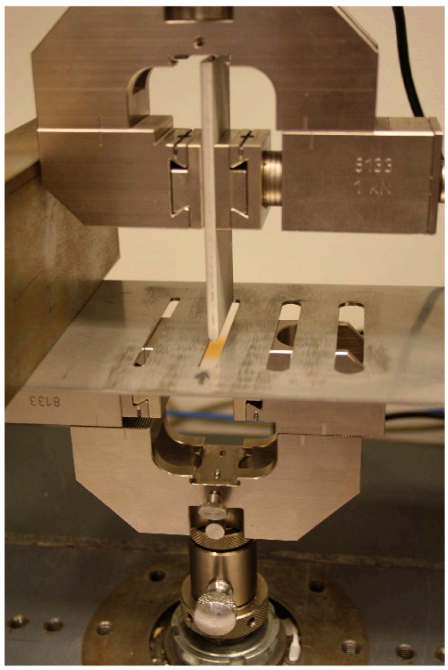

Figure 3.5: Bend Test 1

complicated to implement i ABAQUS. The bend test geometry is identical to the ABAQUS model.

To be able to compare the test with the simulations the test was carried out in a tensile test machine, where the reaction force could be measured. These different test setups with different slot widths, was easily made in ABAQUS as well, for comparison.

In figure 5.4 the radius of the die is 2 mm and the distance between the edges in the whole is 6 mm.

3.2 Fold test

The problem area in the package , fig 1.1b, shows a fold in the material. To simulate this a fold test was invented, an easy test where two plates was pushed together. This test was also easy to simulate in ABAQUS. The test setup can be seen in fig 3.6.

The space between the plates in the initial state was 10 mm and the they were moved together to a reduced space of 0.5 mm The setup in the tensile machine made it possible to get data for Load and Deformations plots.

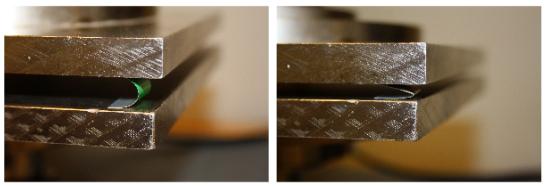

(a) Unfolded (b) Folded

Figure 3.6: The Fols Test

3.3 Investigation of the bend test and fold test

To investigate the bend test and to locate the crack a microtome was used. A microtome is a machine which allows one to cut extremly thin slices of a material. The slices are automatically glued on to a sticky tape and manually added to a piece of glas. This setup allows one to investigate the sample, the slice, in a microscope or an electron microscopy. Thickness of the slices used in this thesis was $50\mu m$. In figure 3.7 one can study a picture from the microscope, the picture is from a 50μm slice and the enlargement is x10.

Figure 3.7: Microtome picture, $50\mu m$ x10

The red ring shows a fracture in the foil and necking of the LDPE.

One can easily understand that very thin slices of a very thin material are brittle and sensitive. There for should one keep in mind that some of the pictures taken with the microscope can hold damage in the material that has been carried out during slicing of the material.

Approach for the conclusions

To make conclusions of the microscope pictures a structured approach is necessary. This approach is described in the list below.

- Thickness for all slices was $50\mu m$
- All slices were treated in the same way and very carefully.
- Ten slices were made for each test specimen, sliced with a space of $250\mu m$ between them.
- The specimens were investigated in the microscope with the ambition to locate cracks and trends for the specimens.

Locate cracks without Microtome
An easy method to quickly locate cracks in this type of package material is to use a flashlight. If the flashlight is placed behind the material and one can observe light passing the material one can be sure of that a crack has propagated through the aluminum. This method is absolute and do not lack reliance like

the microtome method do in manner of damage from the method process. One should take in consideration that white light from a flashlight has bigger wave length that other sorts of light, this means that there can, in theory, exist a crack but it is too small for the white light to pass. In this work there was no time and no need for a other test method than those presented, should one be interested in investigation of smaller cracks one can use a Electron Microsope instead of an ordinary one.

This method was used in a early stage so that one could see that a crack really appears after the material has been folded. After this the fold test was born and the results shows that it did work.

3.4 ABAQUS Model

ABAQUS is a Finite Element Method program based on deformation, consisting of different modules and solution techniques. To create a model in ABAQUS one follows three stages. The first stage, preprocessing, is to create a geometric model in ABAQUS/CAE, this module is similar to a CAD program. In the second stage the preprocessing file is sent to the solver, either the ABAQUS/Standard using an implicit solver or the ABAQUS/Explicit using an explicit solver. In the third stage the results is published in files ready to be post processed. For further information about ABAQUS and its qualities see [12].

3.4.1 Numerical solver

The numerical method used for this case is a dynamic implicit method, a solver available in ABAQUS/Standard. This method is the only dynamic method where XFEM is implemented. See Chapter 3 for further details.

A Quasi-Static stress analyst is used to be able to stabilize the solution with mass-scaling. Mass-scaling is a method that uses the mass inertia by vary the density so that the solution becomes stable.

3.4.2 Load case

To know how big deformation the laminate can suffer in the test rig one can recall beam theory [5]. Modifications are needed when the beam consists of different materials

$$\varepsilon_x(z) = z\frac{1}{R} + C \tag{3.1}$$

$$\sigma_x(z) = E_s(z)\varepsilon_x(z) = E_s(z)\varepsilon = E_s(z)\frac{z}{R} + E_s(z)C \tag{3.2}$$

Where $\varepsilon_x(z)$ is the strain in x-direction, R the curve radius, z is the distance from the inside of the bending radius to the locus for the deformation, $\sigma_x(z)$

the stress in x-direction, $E(z)_s$ Young's modulus in x-direction for material s and C is a constant.

To determine C (3.2) and the following equation is used

$$\int_0^h \sigma dz = \int_0^h E_s \frac{z}{R} + E_s C dz = 0 \tag{3.3}$$

Where h is the thickness of the laminate which is divided into different sections named $z_1 ... z_i$

$$\int_0^{z_i} E_s \frac{z}{R} + E_s C dz = \left[\frac{E_s^1 z_1^2}{2R} + E_s^1 z C\right]_0^{z_1} \dots \left[\frac{E_s^i z^2}{2R} + E_s^1 z C\right]_{z_{i-1}}^{z_i}$$
$$= E_s^1 \frac{z_1^2}{2R} + \left(E_s^1 \frac{z_2^2}{2R} - E_s^1 \frac{z_1^2}{2R}\right) \dots \left(E_s^i \frac{z_i^2}{2R} - E_s^i \frac{z_{i-1}^2}{2R}\right) + C E_s^1 z_1 + C E_s^2 (z_2 - z_1)$$
$$+ \dots + C E_s^i (z_i - z_{i-1}) = 0 \tag{3.4}$$

Gives

$$C = \frac{E_s^1 \frac{z_1^2}{2R} + \left(E_s^1 \frac{z_2^2}{2R} - E_s^1 \frac{z_1^2}{2R}\right) + \dots + \left(E_s^i \frac{z_i^2}{2R} - E_s^i \frac{z_{i-1}^2}{2R}\right)}{E_s^1 z_1 + E_s^2 (z_2 - z_1) + \dots + E_s^i (z_i - z_{i-1})} \tag{3.5}$$

The initial yield stress, σ_{yo}, for the materials is known. This is compared with $\sigma_x(z)$ from (3.1) and (3.2) and a radius at which the material yields can be calculated.

Load Case to initiate movement

To initiate the right movement, in the fold test, of the specimen and to reduce instability a load pressure were set on the left side in the $x-$direction. The pressure was tested and reduced to a minimum to not impact the accuracy of the model.

3.4.3 The adhesive layer

ABAQUS needs the following parameters for the adhesive layer

Parameter	*Description*	*Unit*
K_{ss}	The stiffness of the adhesive layer	MPa
K_{nn}	The stiffness of the adhesive layer	MPa
K_{tt}	The stiffness of the adhesive layer	MPa
σ_{yy}	Maximum normal stress	MPa
τ_{xy}	The maximum shear stress i the xy-plane	MPa
τ_{zy}	The maximum shear stress i the xy-plane	MPa
G_c	Critical Fracture Energy	J/m^2

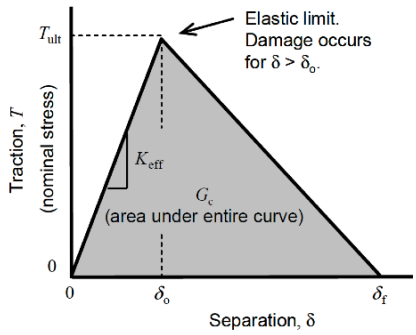

Figure 3.8: Separation law for the cohesive behavior in ABAQUS [6]

One can se in figure 3.8 how these parameters is described in the separation law. With data from the physical tests and a method developed by Kinloch [8] these parameters can be calculated. The method is based on mechanical equilibrium of the peel test.

Kinloch and his colleagues has programmed an Excel document [8] which calculates the fracture energy G_c and the maximum normal stress σ_{yy} for the adhesive layer. The document needs the following physical test parameters

- b The width of the sample
- E Young's Modulus for the peel arm
- P The peel force
- θ The peel angle

If one observes the peel arm like a "infinitely-rigid string" the equilibrium equation takes the following form

$$G_c = \frac{F_{peel}(1 - cos\theta)}{b} \tag{3.6}$$

Together with

$$G = \frac{\sigma \delta_n^t}{2} \tag{3.7}$$

where δ_n^t is the separation in the normal direction, gives

$$\sigma_{yy} = \frac{G_c 2}{\delta_n^t} \tag{3.8}$$

G_c is the fracture energy for the adhesive layer.

In [8] Kinloch also take consideration of the peel arms mechanical impact on the total energy that is needed. For further information of the theory behind [8] see [9]

3.4.4 Element and Mesh

The elements used in the model was 4-node bilinear plane stress element and the geometric order for the element is linear (in ABAQUS named $CPS4$). Plane stress was used due to the two dimensional case and the linearity was chosen do to that XFEM in ABAQUS can not handle elements of quadratic geometric order. No reduced integration is used do to problems with hour glassing, with reduced integration one can increase the accuracy of the system do to the reduced system stiffness [10]. In this case the reduced integration resulted in a collapse of the board in the TFA material, do to it's orthotropic behavior, there for a full integration was chosen. For further information about recommended elements for different analyses see [12] or [10].

The mesh were refined in the area where the fold appear for reduced computational time and because the other areas were not to be investigated. The mesh can be seen in figure 3.9

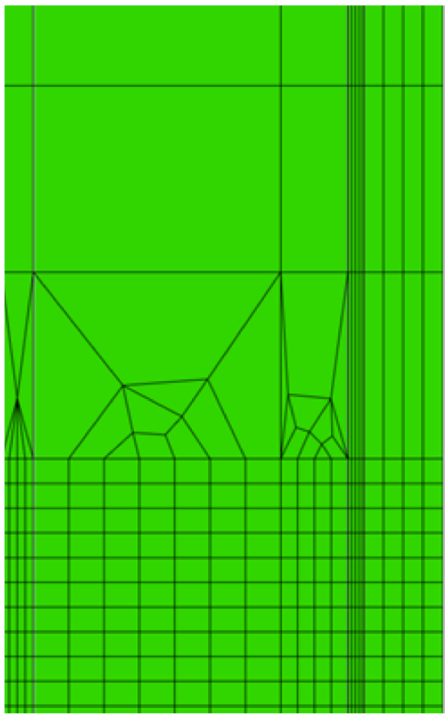

Figure 3.9: The Mesh

3.4.5 Material model

The LDPE layers are approximated as linear elastic, this is a approved approximation because of it's lack of stiffness relative the board and the aluminum.

The board is simulated as an anisotrpic (orthotropic) material. This is implemented both in a elastic and a plastic manner in ABAQUS. In the Material

Editor under Elastic ABAQUS asks for Young's modulus, Poisson's ratio and the bulk modulus in all three directions of the local Cartesian system. In this simulation the third direction, z, is not affected because the simulation is in 2D. The following parameters was implemented.

Parameter	*Description*	*Input*
E_1	Young's Modulus i x-direction (MPa)	4283
E_2	Young's Modulus i x-direction (MPa)	42.8
E_3	Young's Modulus i y-direction (MPa)	1
ν_1	Poisson's ratio $(Index)$	0.01
ν_2	Poisson's ratio $(Index)$	0.01
ν_2	Poisson's ratio $(Index)$	0.01
G_{12}	Bulk Modulus (MPa)	428
G_{13}	Bulk Modulus (MPa)	1
G_{23}	Bulk Modulus (MPa)	1

The aluminum is implemented as linear elastic until it yields, then the aluminum holds a plastic behavior with isotropic hardening. To implement this ABAQUS needs the yield stress and some points on the stress/strain curve after the yield stress. The following parameters was implemented in the Material Editor in ABAQUS.

$YieldsStress(MPa)$	$PlasticStrain$
35	0
36.737	0.00208737
38.0415	0.00269147
39.346	0.00339994
40.6505	0.00422728
41.955	0.00518942
43.2595	0.00630373
44.564	0.00758916
45.8685	0.00906622
47.173	0.0107571
48.4775	0.0126857
49.782	0.0148776
51.0865	0.0173602
52.391	0.0201627
53.6955	0.0233161
55	0.0268531

Both the board and the aluminum parameters is taken from studies and tests at Tetra Pak, they were taken from Ulf Nyman and Eskil Anderasson.

3.4.6 Parameter Study

The parameter study is based on variation of the adhesion layers and variation of the stiffness in the LDPE. During the study the reaction force and the maximum strain in the aluminum was measured. The reaction force is interesting because this describes the resistance against folding and the maximum strain is a measure

of the impact of the material. Due to ideal elastic-plastic material models will the stress only reach a fixed value but the strain will keep increase why the strain is more interesting.

- Normal adhesion is based on the measured values from the adhesion test, this adhesion is given the name L in the result chapter.
- Higher adhesion is two times L, $2G_c$ and $2\sigma_{max}$, this has been given the letter H
- Extreme adhesion has been given the TIE in the result chapter to indicate that a TIE constraint has been used instead of surface based cohesive behavior
- The variation of the LDPE is either the normal value of $300MPa$ or the higher value of $400MPa$

3.4.7 The Final Model

All steps in ABAQUS are now explained and how the whole model looks like, in a deformed stage, can be seen in figure 3.10.

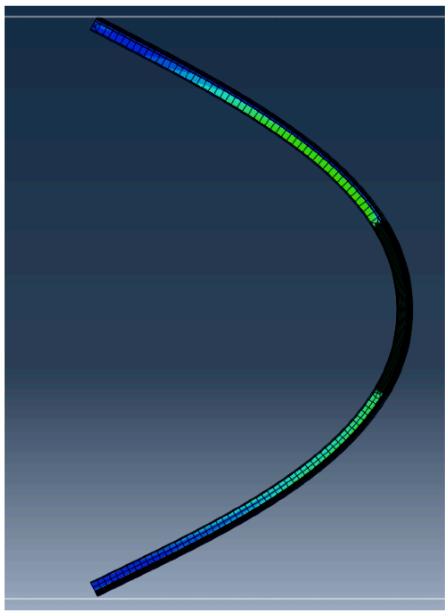

Figure 3.10: The Model

Building the final numerical model

The numerical crack model are based on the geometry of the fold test, presented in section 3.2, see figure. To build a proper model the work was carried out systematic with different stages where different parts and physical phenomena was implemented.

1. Develop the geometry, load case and boundary conditions of the model.
2. Implementation of the different materials. One by one with surface based cohesive behavior so one can see that the model work and to detect early errors and difficulties.
3. Testing of different meshes and loads.
4. Implement material models one by one.
5. Implementation of XFEM.

Geometry and load

The geometry was set like this with consideration that the geometry should be easy to implement both i ABAQUS and in a physical test. The basis of the geometry is two plates that are pushed together as the material is folded between them. To initiate the proper path for the material a small pressure pushes the standing material into it's right path. This pressure also reduce the risk for instability with this kind if load case, it can be compared with Euler's buckling cases.

Boundary conditions

When setting the boundary conditions the goal was to simulate the reality while numerical and mechanical difficulties was tried to be avoided. The upper parts surfaces of the specimen was coupled together to one point by a couple constraint in ABAQUS, this point was then locked only in the x-direction so that the specimen could both rotate around the locked point and translated in the y-direction.

The lower parts of the specimen was locked together to a point by coupling in ABAQUS exactly like the upper part but the lower parts coupled point was also locked int the y-direction but not in a rotational manner.

XFEM implementation in ABAQUS

In ABAQUS one first need to create the XFEM crack editor and give the crack a geometry. After this one creates an interaction named XFEM Crack Growth and makes a coupling to the already existing crack one created earlier. The last step is to give the material in the section where the crack can appear the right material behavior, this is done by defining a Maxps Damage with both Damage Initiation and Damage Evolution in the material editor. For further information about Damage Evolution and Initiation see Chapter Theory or [12].

Convergence problems in XFEM

The discontinuities in the enriched area in a XFEM simulation can some times lead to convergence failure even if a well refined mesh is used or the damage parameters are set realistic [15]. The XFEM method is in a computional manner harder than the ordinary Finite Element Method because of its singularities. Do to these numerical problems some parameters in ABAQUS need to be changed. The parameters are changed in the General Solutions Controls Manager, the number of attempts per increment I_A is set to 10 or more and the box for Discontinuous Analyses are toggled on. To improve the convergence even more

one can change some material parameters and set stabilization for the damage. These parameters are changed in the Material Editor, the stabilization for Damage and the tolerence for damage is changed under sub option for Maxps Damage. For further information about these parameters see [15] and [12].

If none of the above methods work one can prove to refine the mesh. After different attempts in ABAQUS one saw that the convergence can be achieved with a more refined mesh, both horizontal and vertical.

Chapter 4

Results

4.1 Results from the bend test

The results from the bend test is reported with pictures from the microtome. Figure 3.7 shows a crack in the material. Zones like this were searched in the following microscope pictures. No such zones could be recognized which led to development of a new test method, the fold test. The test specimens was also investigated with the flashlight test method.

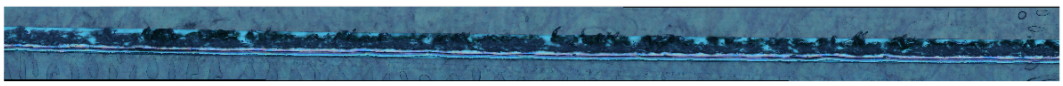

Figure 4.1

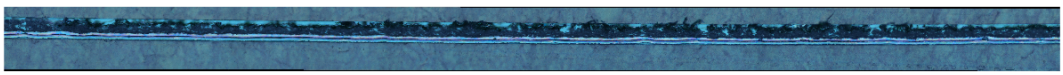

Figure 4.2

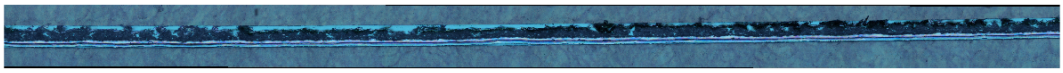

Figure 4.3

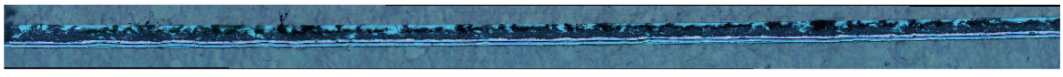

Figure 4.4

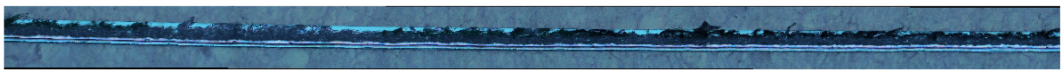

Figure 4.5

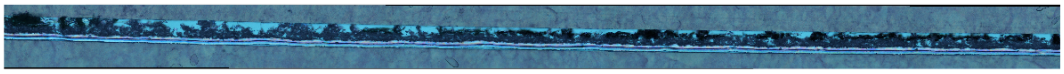

Figure 4.6

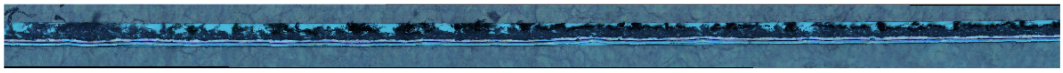

Figure 4.7

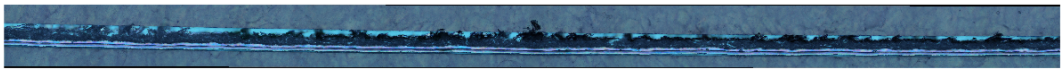

Figure 4.8

Figure 4.9

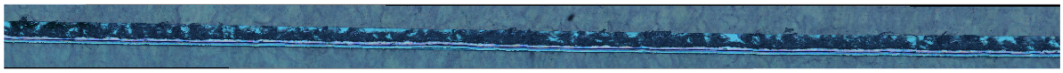

Figure 4.10

4.2 Results from the Fold Test

The test specimens was investigated with a flashlight before they were investigated with the microtome. Motivation for these tests was to ensure that a crack really did appear after the fold test, which it did. Figure 4.11 shows failure in the material after the fold test.

To compare the reaction force between the simulation and the physical tests the maximum force from the tests were measured and a mean value was calculated. The difference in reaction force between the simulation and the physical tests can be explained because of the increased stiffness due to the full integration. Tests results can be seen in the table bellow.

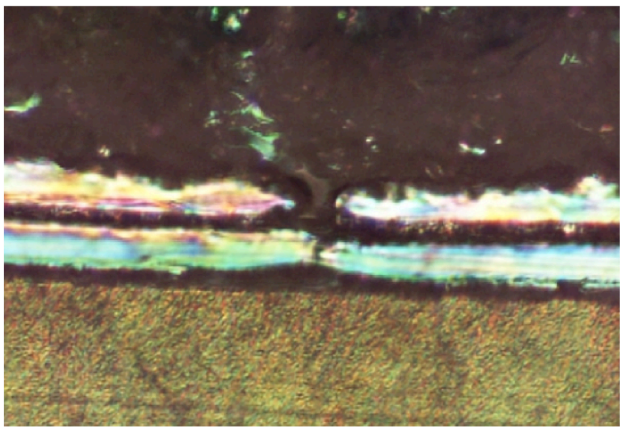

Figure 4.11: Failure after the Fold Test

$Test$	$Max.Reac.Force(N)$
1	4.662
2	4.417
3	4.304
4	5.066
5	4.999
6	4.485
7	4.892
8	4.803
9	4.391
10	4.971
$Meanvalue$	4.699

Verification of the Fold Test

To verify the simulation model displacement- and force plots from the simulations was compared with plots from the physical tests. In figure 4.12 one can see these plots compared, the simulation plot is Run 1 in the table bellow.

Figure 4.13 shows that a real physical phenomena appears in the simulation as well.

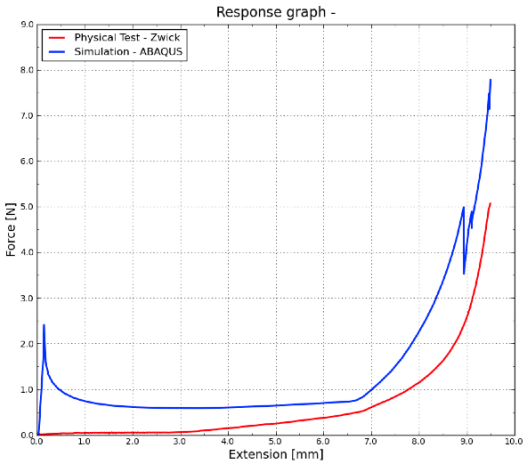

Figure 4.12

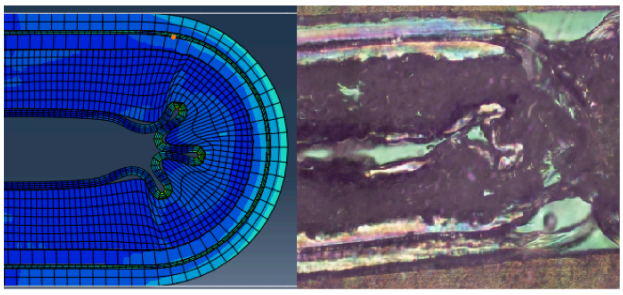

Figure 4.13

The Parameter Study

Different variation has been carried out, these can be seen in the tables bellow. Here are the different reaction forces and the different strains presented as well.

Table shows the parameter study with variation of the adhesion.

Run	*Ins-Foil*	*Foil-Lam*	*Board-Lam*	*Force (N)*	*Strain (%)*
1	L	L	L	7.77415	0.174152
2	L	L	H	7.77415	0.174152
3	L	H	L	7.77415	0.174152
4	L	H	H	7.77415	0.174152
5	H	L	L	7.77415	0.174152
6	H	L	H	7.77415	0.174152
7	H	H	L	7.77415	0.174152
8	H	H	H	7.77415	0.174152
9	L	L	TIE	8.23257	0.20621
10	L	TIE	L	823257	0.195444
11	TIE	L	L	7.98751	0.146813

The location for the maximum strain in Run 1 can be seen in figure 4.14. The picture is taken from Run 1 because this model is based on the measured adhesion values.

Figure 4.14: Location for Maximum Strain

Table shows the parameter study with variation of the stiffness in the LDPE layers.

Run	*Ins.(MPa)*	*Lam (MPa)*	*Adhesion*	*Force (N)*	*Strain*
12	300	300	L	7.77415	0.174152
13	300	400	L	7.92772	0.170073
14	400	300	L	8.23905	0.154461

4.3 Results from the XFEM simulation

No real results was carried out by the XFEM simulation. The reader could have help from Chapter 3 when implementing the XFEM in other models. This is why the XFEM field still serves a spot in this thesis.

4.4 Results from Microtome Pictures

Ståhle *et al* has written an article [16] about necking in laminates of LDPE and aluminum linked to the adhesion. In this article there were no physical tests done and no real pictures, only FEM calculations and simulations. The results founded during this study shows and proofs the theory in Ståhle *et al* article [16].

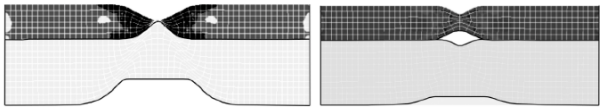

Figure 4.15: Picture from [16]

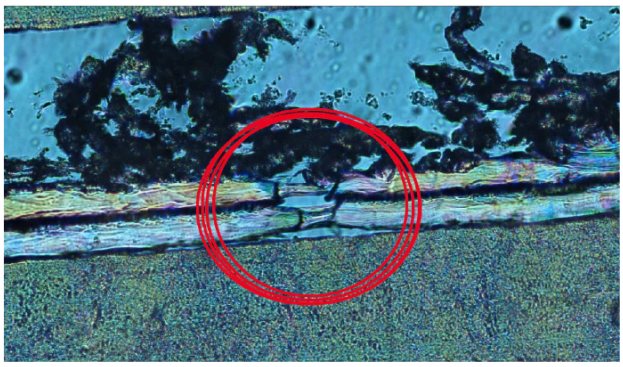

Figure 4.16: Microtome picture

One can easy see the similarities between the figure 4.15 and figure 4.16

4.5 Discussion

Some of the differences in the verification can be explained out from physical phenomena and numerical problems. The load peak in the beginning of the simulation curve in figure 4.12 can depend on the instability that the system holds in the beginning of the bending, just like an Euler buckling case. The fluctuation of the load at the end of the compression can be explained with collapse of the adhesion between the board and the outside LDPE, or by the boards material model.

The choice of full integration can affect the stiffness of the material, this can be the reason for the difference in the maximum load between the physical tests and the simulation.

Some of these differences could have been reduced by calibrating the model or to make better physical tests that were more like the boundary conditions in the simulation. Maybe one could have found a better solution to reduce the hour glass phenomena than to use full integration. If this would be possible maybe the difference in reaction force could have been eliminated or reduced.

4.6 Conclusions

The ultimate case is to have a maximum reaction force to increase the fold stiffness in the material and to minimize the strain to reduce the risk for cracks in the aluminum. In the tables for the parameter study it seems to be the cases with extreme adhesion between the inside and the foil and a stiffer inside LDPE that is the best solution to reduce cracks and big bend radius.

4.6.1 Future work

Through out my work I found many areas that needs further investigation, areas that could be done as small tasks or as new master thesis. Because of the limited time these areas could not be investigated but there significance is not neglectable.

The Mesh

The mesh can be seen in figure 3.9 and the asymmetry in the elements is obvious. This asymmetry can contribute to stress and force differences in the ares where the asymmetry is located and the maximum strain location can be explained due to this mesh. A more refined mesh could also be interesting to investigate, and how this could impact the reaction force and maximum strain.

The Initial Load

The initial pressure in the model can affect the reaction of the model, an alternative to this small pressure can be an initial deformation of the specimen instead of the initial pressure.

Material behavior

The material models that is used is simplified and could be both expand to involve hardening behavior and delamination of the paper board. The delamination could be modeled with surface based cohesive behavior, cohesive elements or just with layers in the paper that not is tied together.

Simulation of a adhesion test

The biggest area that needs further investigation is the adhesion test. Adhesion is a very hard physical phenomena to measure and to quantify. The best way to verify the adhesion test should be to model an exactly peel test in ABAQUS that was used to measure the adhesion, see Chapter 3. With a modeled peel test the physical test could be used to calibrate the model in ABAQUS and help to quantify the adhesion parameters. This implementation is not an easy task and could be carries out as an new master's thesis. The implementation is then easy to use and implement in the model used in this thesis.

Bibliography

[1] S. Krenk: *Non-linear Modeling and Analsis of Solids and Structures*, Cambridge University Press,(2009)

[2] N. Saabye Ottosen, M. Ristinmaa: *The Machanics of Constitutive Modeling*, Elsevier,(2005)

[3] S. Bordas, A. Legay: *X-FEM Mini-Course*, Lausanne,(2005)

[4] AJ. Kinloch, C.C. Lau, J.G. Williams: *The peeling of flexible laminates*, Department of Mechnical Engineering, Imperial College of Science, Technology and Medicine, London (1994)

[5] C. Ljung, N. Saabye Ottosen, M. Ristinmaa: *Introduktion till Hållfasthetslära, Enaxliga tillstånd*, Studentlitteratur, Lund (2007)

[6] T. Diehl: *Modeling Surface-Bonded Structures with ABAQUS Cohesive Elements: Beam-Type Solutions*, DuPont Engineering Technology, Wilmington (2005)

[7] F. Nilsson: *Fracture Mechanics from Theory to Applications*, Royal Institute of Thechnology, Stockholm (2001)

[8] AJ. Kinloch: *Excel document ICPeel Digitised Stress-Strain 2007*, http://www3.imperial.ac.uk/people/a.kinloch, (2007)

[9] LF. Kawashita: *The Peeling of Adhesive Joints*, Ph D Thesis University of London, (2006)

[10] N. Saabye Ottosen, H. Petersson: *Introduction to the Finite Element Method*, Prentice Hall Europe (1992)

[11] B. Sundström: *Handbok och formelsamlig i Hållfasthetslära*, Royal Institute of Thechnology, Stockholm (1999)

[12] ABAQUS: *Documentation*, 6.10

[13] M. Norrlander: *CRACK PROPAGATION IN FIXED CALLIPER BRAKE DISCS*, Master's Thesis at the Division of Solid Mechanics at Lund Institute of Thechnology (2004)

[14] J. Lönn, J. Navréd: *DROP TEST OF A SOFT BEVERAGE PACKAGE Ű EXPERIMENTAL TESTS AND A PARAMETER STUDY IN ABAQUS*, Master's Thesis at the Division of Solid Mechanics at Lund Institute of Thechnology (2006)

[15] Simulia Dessault Systemés: *Improving Convergence in XFEM Analyses*,

[16] P. Ståhle, C. Bjerkén, J. Tryding, S. Kao-Walter: A STRONG TOUGHENING MECHANISM IN AN ELASTIC PLASTIC LAMINATE: *Proceedings of the 28th Risø International Symposium on Materials Science*,

Chapter 5

Appendix

5.1 Data from adhesion tests

To get the force for document [8] one have to multiply the dimensions bellow, these are in (N/m).

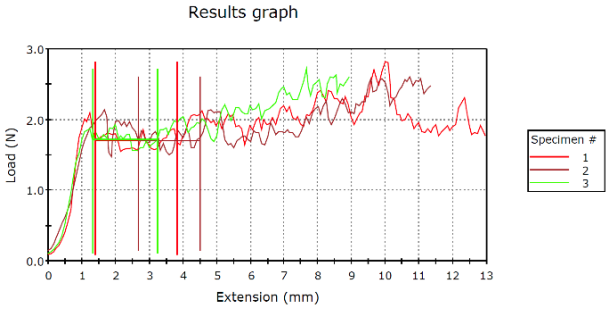

Figure 5.1: Graph, 180^o Peel test for the decor and board

	Average Load/Width (N/m)
1	113
2	113
3	114
Mean	114
Std	0.69
CV	1
Max	114
Min	113

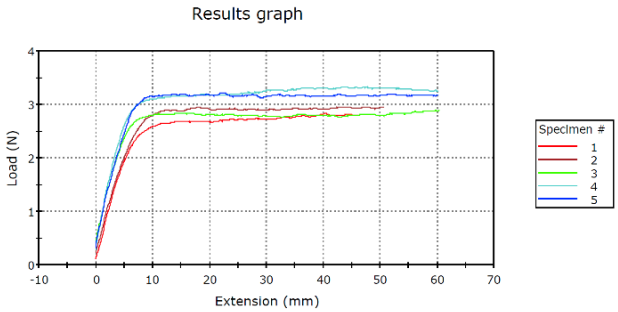

Figure 5.2: Graph, 180^o Peel test for the inside LDPE and the Foil

	Average Load/Width (N/m)
1	177
2	193
3	188
4	210
5	211
Mean	196
Std	14,6
CV	7
Max	211
Min	177

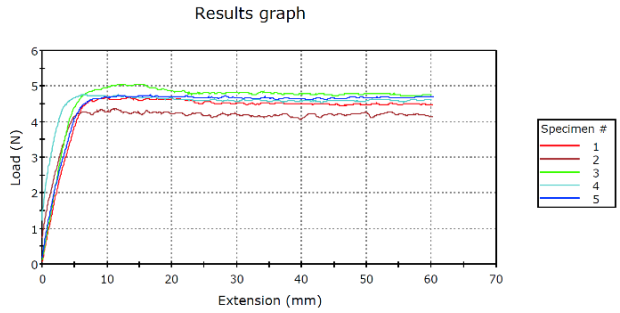

Figure 5.3: Graph, 90^o Peel test for the inside LDPE and the Foil

	Average Load/Width (N/m)
1	308
2	284
3	332
4	312
5	314
Mean	310
Std	17.03
CV	5
Max	332
Min	284

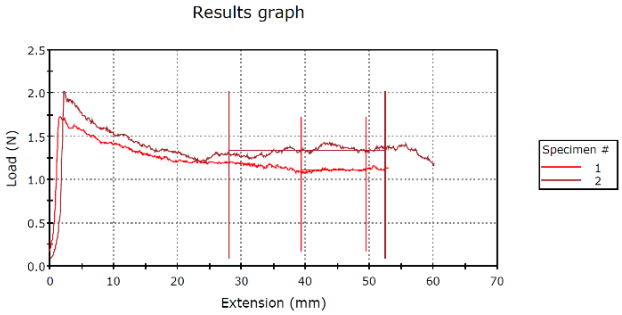

Figure 5.4: Graph, 180^o Peel test for the inside Laminate and the Foil

	Average Load/Width (N/m)
1	74
2	89
Mean	81
Std	10,7
CV	13
Max	89
Min	74

5.2 Plots from the parameter study

The following plots are compared with the physical test. The material properties can be seen in the run tables in Chapter 4.

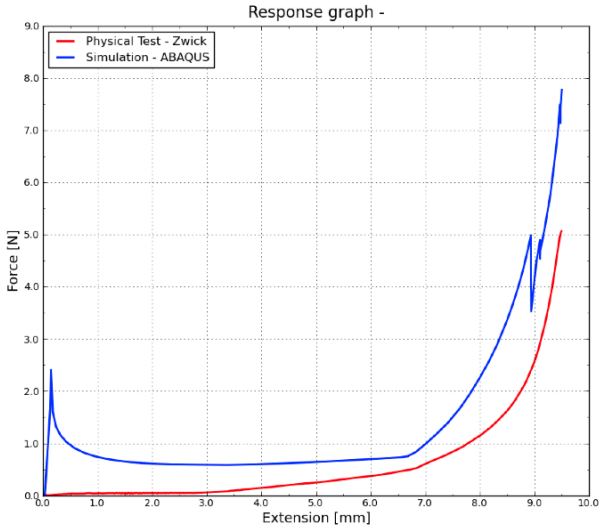

Figure 5.5: Run 1

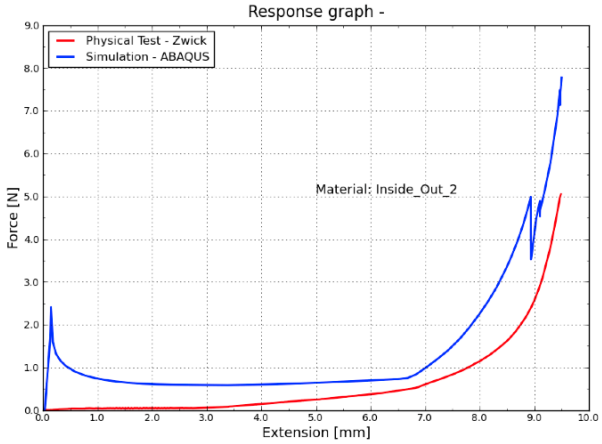

Figure 5.6: Run 2

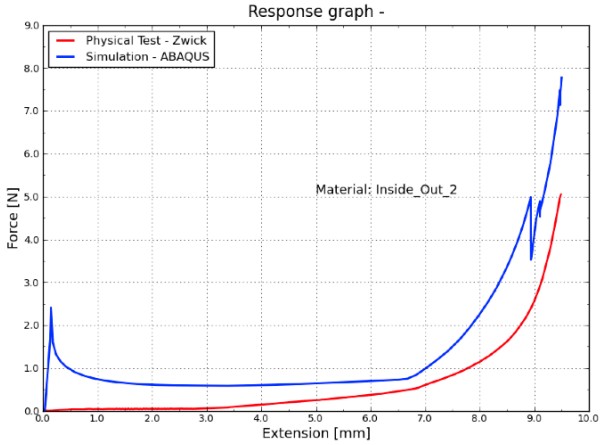

Figure 5.7: Run 3

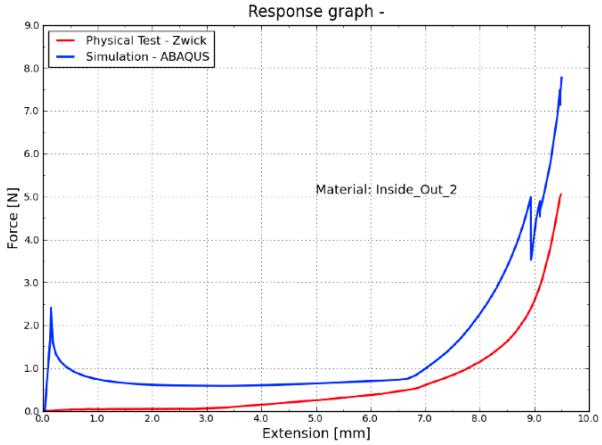

Figure 5.8: Run 4

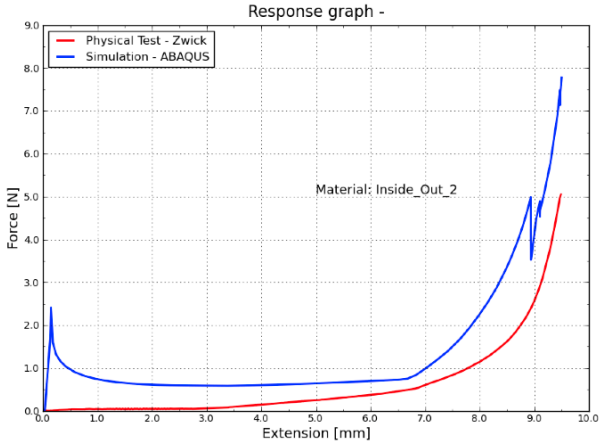

Figure 5.9: Run 5

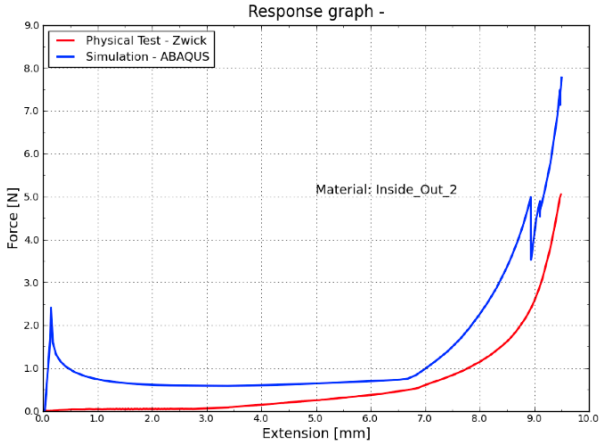

Figure 5.10: Run 6

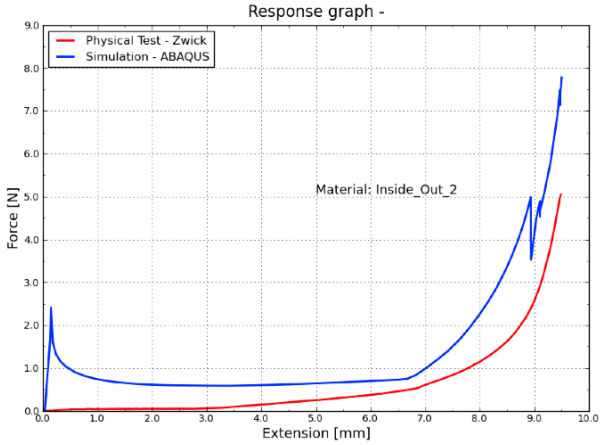

Figure 5.11: Run 7

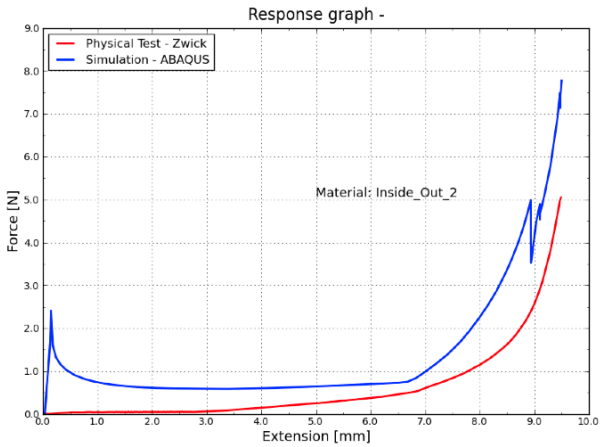

Figure 5.12: Run 8

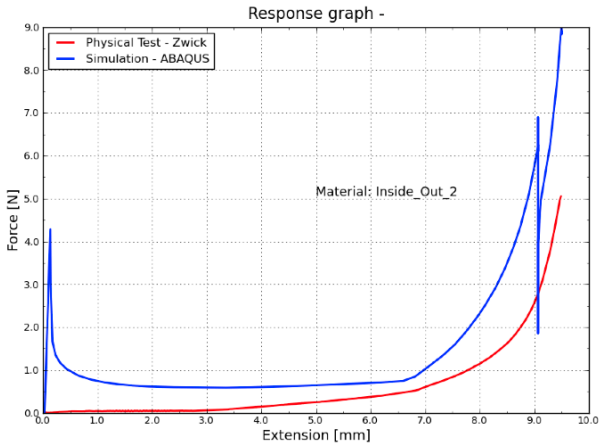

Figure 5.13: Run 9

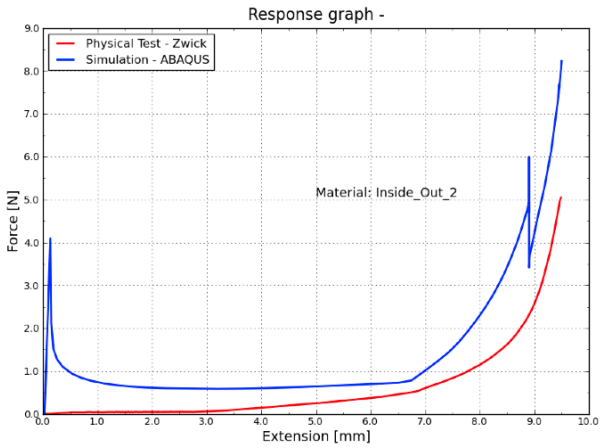

Figure 5.14: Run 10

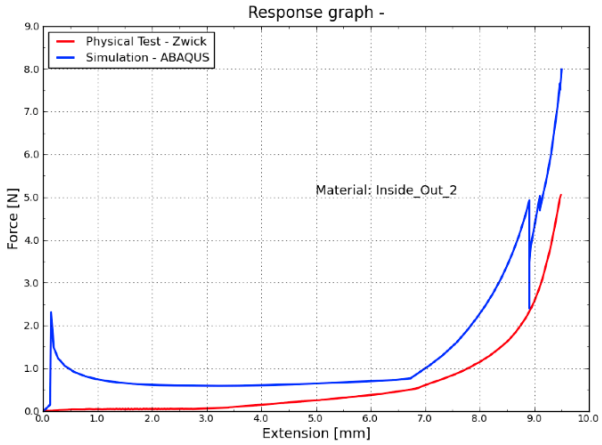

Figure 5.15: Run 11

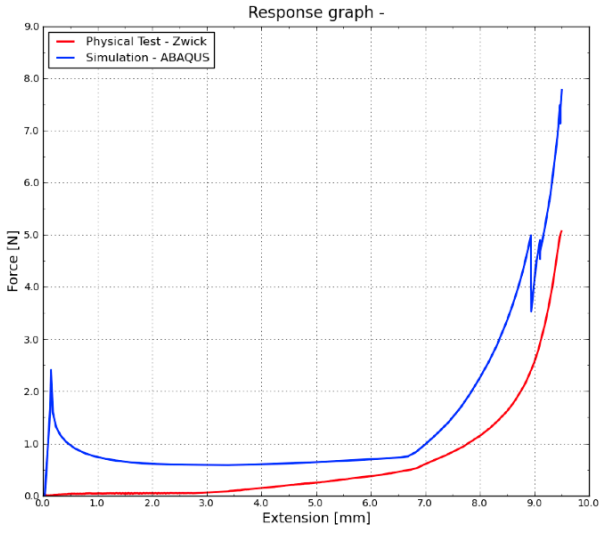

Figure 5.16: Run 12

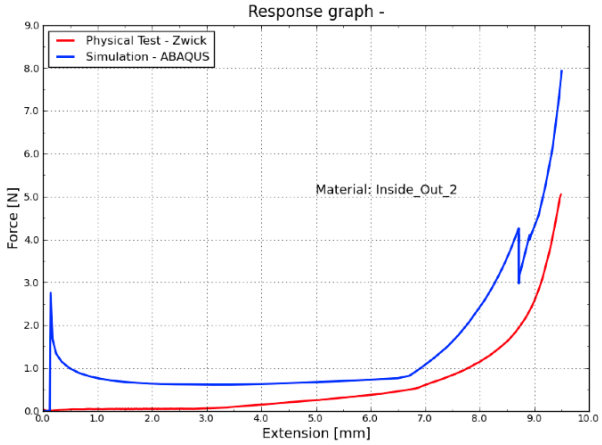

Figure 5.17: Run 13

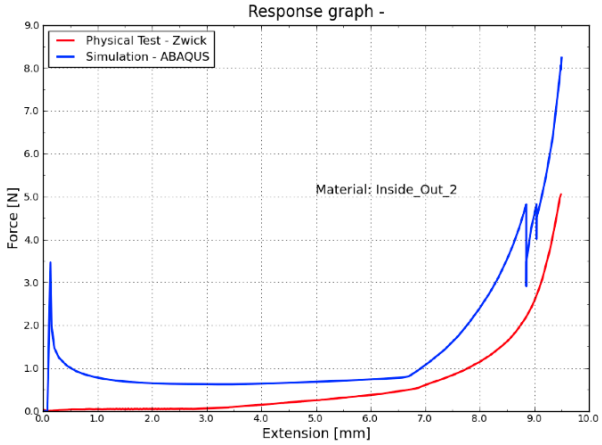

Figure 5.18: Run 14